

Diffraction patterns correlation with shape and structure of imprint objects

M. MIHAILESCU*, A. PREDA, D. COJOC^a, E. SCARLAT, L. PREDA

Physics Department, University "Politehnica" of Bucharest, Romania

^aTASC-NNL-INFM (National Institute for the Physics of Matter) at Elettra Synchrotron

Light Source, Lilit Beam-line, Trieste, Italy

Analysis of optical diffraction pattern of natural or virtual objects is an actually problem which has important applications. We realized the correlation between diffraction patterns from imprinted objects with different shapes, structures and sizes. An iterative algorithm based on Fourier transform for far field written in MATLAB is used to design computer generated hologram (CGH) in a different number of equidistant phase-levels patterns, which produces the desired image in far field. Spatial light modulators (SLM), two-dimensional electrically addressable devices, are used in experimental setup in order to modulate the phase of a wave front from a monochromatic plane wave. Through the diffraction pattern obtained experimentally with CGH and SLM, we show that the shape of the objects is of less importance than the structure. The shape is modified by different geometrical figures, and the structure is periodical, with or without defects. We use this method to study different imprint objects. By correlation profile we remark the distinction in the shape and structure of different sample.

(Received November 2, 2006; accepted February 28, 2007)

Keywords: Computer generated holography, Correlation function, Diffraction pattern, Spatial light modulator, Imprint objects

1. Introduction

The diffraction pattern given by a sample generally provides information which depends on several parameters: shape, structure, phase contrast, dimensions, defects, wavelength, polarization, incident and observation angles. Using these informations, we may improve the recognition of a diffraction object in certain circumstances. The small cracks or cavities can be conveniently analyzed by their diffraction pattern [1], also same natural sample or 3D objects [2]. In recent applications the diffraction pattern from all particles illuminated is used to study a dynamic optically-bound assembly of spherical colloidal particles [3]. There the relative intensities and the profile of the diffracted beams contain much valuable information, such as the lattice constant, crystal orientation or defect properties of the assembly. Correlation analysis is a powerful tool that allows detecting small changes in a particular diffraction pattern, corresponding of changing in diffraction sample (DS).

Starting from the shape and structure of the sample, we generate on computer a model - DS in role of the diffraction element (DE), which provides a way to automatically generate complex and rapidly changing laser illumination patterns in the far-field. Diffraction element's geometry can be dynamically changed experimentally using a phase-only spatial light modulator (SLM), which is an optoelectronic device useful for the application in optical image processing, programmable diffraction optics and adaptive optics [4, 5].

In the second part of this paper, we present theoretical considerations about iterative algorithm for CGH design.

Also, we present the theoretical basis for changing the extraordinary index of refraction when on SLM is electronically addressed different gray levels.

In the third part of the paper, we present the experimental results obtained in the study of imprint objects and different arrangements of CGH (multiple objects in parallel, in series, differences). Here, we take into account the microstructure of the imprint objects, and model it as a grating, with experimentally measured diffraction pattern sequences from a 600 x 800 pixel phase-only SLM. The simulation results of power spectrum density (PSD) and the correlation for special diffraction sample are plotted and presented in section four. Examples of correlation maps from different imprint objects are interpreted and the differences are relieved. Correlations between matrices allow comparing a set of shapes and structures.

The diffraction parameters as derived from our correlation analysis between diffracted sample and far-field diffraction pattern, as well as the shape resolution, are presented. We end with conclusions and discussions.

2. Theory

Through its construction, SLM has a pixelated structure and the diffraction pattern is repeated in many orders, which leads to a decrease of the efficiency. The low spatial resolution of electronically addressed SLMs permits to restrict the analysis of the displayed diffraction elements to the scalar theory [6]. Goodman [7] demonstrated that in the particular case when the DE is illuminated by monochromatic, unit amplitude, normal

incident plane wave, the transmission function of the DE is related by a Fourier transform to the field in the image plane.

We consider here the usual case where the D plane is the Fourier plane (spatial frequencies) of the diffractive element on SLM, and the object plane E is the physical plane (screen plane) of the reconstructed image. For DE design, we start with a given desired image in signal window [8], boarded with zero elements to form in MATLAB an $N \times N$ matrix ($N=2^n$, $n=1,2,3,\dots$). To create the initial function $t_E(x, y)$ in E plane, we multiply this amplitude matrix $A_E(x, y)$ with a phase factor $\varphi_E(x, y)$, which is initially generated random, or constant:

$$t_E(x, y) = A_E(x, y) \cdot \exp(i\varphi_E(x, y)) \quad (1)$$

where x, y are the coordinates of the centre of each pixel.

Its inverse bi-dimensional Fourier transform:

$$\begin{aligned} T_D(p, q) &= \mathcal{IF}(t_E(x, y)) = \\ &= A_D(p, q) \cdot \exp(i\varphi_D(p, q)) \end{aligned} \quad (2)$$

brings us the transmission function in D plane, where $p = x/\lambda L$, $q = y/\lambda L$ are the spatial frequencies in D plane, L is the distance between D and E plane, λ is the wavelength of the incident wave. Because SLM is an optical device which modulates the phase of the incident wave, we must put some constraints: $A_D(p, q) = 1$, for ideal case and the phase can take only maximum eight distinct values, by constructive reason, so we discretized the phase function $\varphi'_D(p, q)$ and the total transmission function in D plane becomes:

$$T'_D(p, q) = \exp(i\varphi'_D(p, q)). \quad (3)$$

Its direct Fourier transform brings us in E plane, where (with special function from MATLAB) we can separate the phase function which we keep and the amplitude function which is replaced with initial amplitude $A_E(x, y)$ from the desired image. In this way we compute the new function in E plane and start an Iterative Fourier Transform Algorithm (IFTA) [9] following the same steps described earlier. The aim is to obtain the phase function in D plane which we apply on SLM and formed in E plane a closer intensity distribution to the desired image. Different steps of this algorithm can be changed to obtain a better convergence and diffraction efficiency [10].

In MATLAB, the phase function $\varphi'_D(p, q)$ is a bi-dimensional (800x600 pixels) distribution of maximum eight gray levels between 0 and 256 in RGB mode, which we apply on SLM. Each of them introduced a different

value of the potential V_{rms} which is electronically addressable on each cell of the SLM. The applied potential is a linear function of gray levels for our 8-bit video digitizer and drive electronics (the producer gives $V_{rms} = 0,5V$ for white and $V_{rms} = 4,5V$ for black).

The tilt angle θ of the molecules in each cell depends of the applied voltage [11]:

$$\tan\left(\left(\frac{\pi}{2} - \theta\right)/2\right) = \exp\left[-\left(\frac{V_{rms} - V_t}{V_0}\right)\right] \quad (4)$$

where V_t is the threshold voltage below which no tilting of the molecules occurs and V_0 is the excess voltage. If $V_{rms} = V_t$ then $\theta = -\pi/2$ and the liquid crystal molecules are twisted the angle given by construction reason. When $V_{rms} = V_0 + V_t$ the value for θ become $\arctan(\pi/2 - 2/e)$.

The tilting of LC molecules causes a reduction in the effective extraordinary refractive index

$$\frac{1}{n_e^2(\theta)} = \frac{\cos^2(\theta)}{n_e^2} + \frac{\sin^2(\theta)}{n_o^2} \quad (5)$$

where n_e and n_o are the refractive indexes of the extraordinary and ordinary component without applied voltage. The real phase shift which is seen by the incident wave front of monochromatic, unit amplitude plane wave, is

$$\varphi_{real}(\theta) = \frac{2 \cdot \pi \cdot d \cdot (n_e(\theta) - n_o)}{\lambda} - \alpha_o = \beta - \alpha_o \quad (6)$$

where d is the thickness of the liquid crystal layer, β is the birefringence and α_o is the angle between the polarization direction of incident wave and optical axis of SLM. The discretized phase matrix φ'_D which is obtained with IFTA, is a gray levels map and its corresponded V_{rms} map is applied on SLM, which forms the refractive index map for incident wave.

3. Experimental results

In our experimental setup, after He-Ne laser we put a telescope, the SLM and a CCD situated at distance L . The images are recorded on CCD in the same conditions and are processed on computer in MATLAB. Only the +1 -1 diffractive orders are cropped from the whole image.

We use a twisted nematic LCD from Sony Model LCX016AL, with 26,6x20mm active area, with a VGA graphic card resolution (800 columns and 600 rows active pixels), 32 μ m pitch, 200:1 contrast ratio, 60Hz image frame rate, nearly phase only modulation, acceptable response time (~ 5 ms), increased fill factor, less intensity in

higher diffraction orders, more efficient (more than 70% in first order).

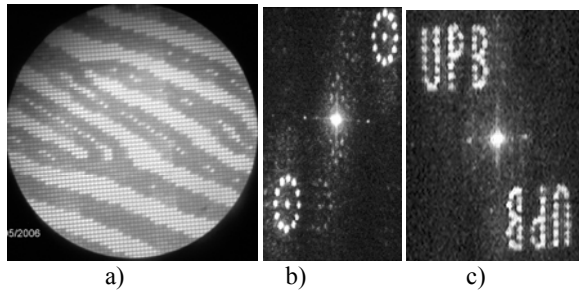


Fig.1. a) The phase matrix on SLM optical microscopic photograph and b-c) diffractive pattern from two different CGH designed by IFTA.

With iterative algorithm described in the second paragraph, we generated two phase DE matrix (Fig. 1a) which create in far field the desired image: a circle formed from points and a logo UPB (Fig. 1.b-c).

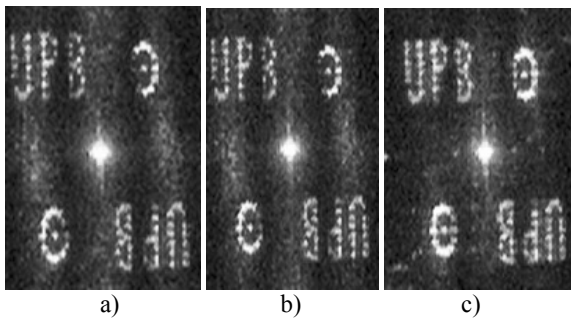


Fig. 2. Diffractive pattern from two CGH calculated by IFTA and some operations between them a) the sum, b) the difference, c) serial arrangements

With these two matrixes we computed in MATLAB three new matrixes with distinct operations: a) sum element by element, b) difference element by element, c) a serial arrangements (a new matrix which has the first 600x400 elements from CGH to make UPB and the last 600x400 elements from CGH to form circle). The reconstruction in E plane gives us both desired image: circle and UPB with the same intensity, clarity and spatial distribution, the distinction is in noise generated around (Fig. 2). When we start IFTA with random initial phase distribution in E plane, the noise is grater than the case when we start with constant initial phase.

In the second part of the experiment, we want to study the diffractive pattern in E plane when we put a given DS on SLM. So, we start with simple models on SLM like vertical or horizontal, equally distant, black and white stripe with different number of pixels. The diffractive pattern is formed by a collinear points disposed horizontal or respectively vertical. The numbers, intensity and positions of points depend from the thickness of the stripe.

The second simple model is a chess table with equally black and white squares. The diffractive pattern in 0-th order show that the position of the points depends by the dimension of the square.

From a diffractive sample formed by black hexagons on white background we obtain a pattern with a spots in the corner of a multi-rectangle shape. The arrangements of the spots in a cross with the 0-th order in center are from the row and columns arrangements of the hexagons. The other points in diffractive pattern are given by the hexagonal shape of the imprint sample.

The next step is the analysis of the diffractive pattern formed by an unknown imprint object with different letters or numbers disposed on rows and columns. The diffractive pattern keeps the central arrangements of the spots in a cross from the row and columns of the imprint sample. The other spots are symmetrically arranged around the cross, but the arrangement is different for each letter (Fig. 3 a-b). Our aim is to detect what DS form this diffractive pattern.

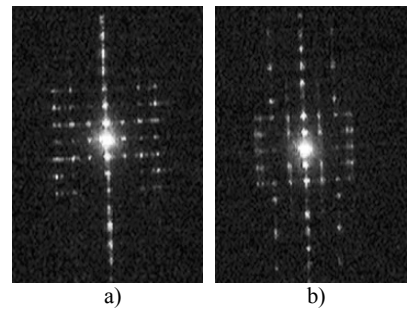


Fig. 3. Experimental diffractive pattern in E plane when the DS is an array of letter.

4. Simulation results

We apply IFTA to design the computer generated hologram from the desired image. We start with the desired image in E plane (Fig. 4a) and the phase reconstructed in D plane is in Fig. 4b. On this phase matrix, we add some periodical defects (white grid), in order to study their influence. In E plane appear both diffractive patterns, as in experiment but for 40%, 20% 8% 4% defects from whole area, the normalized intensity in desired image is respective 0.2, 0.3, 0.35 0,85 for 10 pixels stripes. The width of the defect stripes is more important than their number.

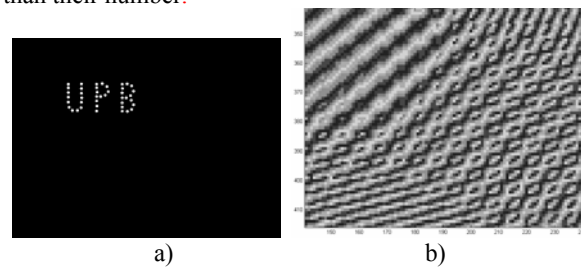


Fig. 4. a) Desired image b) Phase profile in D plane-simulation.

When we start with a given DS in D plane, we study the diffractive pattern in E plane with the aim to compare them and recognize each characteristics (besides background, noise, another DE) or properties (dimensions, shape, periodicity, defects). Again, the intensity distribution in E plane $I_E(x, y)$ is related with the transmission function of the DS $T_D(p, q)$ by its Fourier transform. To determine how many power is in each discrete pixel in E plane, we computed in MATLAB power spectrum density (PSD):

$$PSD(x, y) = \{abs[\mathcal{F}(T_D(p, q))]\}^2 \quad (7)$$

However, the CCD on the image plane does not record the Fourier transform, but the PSD. In order to measure the similarity of two different DE, we can compute cross-correlation, commonly used to find features in an unknown DE by comparing it to a known one. In MATLAB we computed them using the theorem [7]:

$$\mathcal{F}(cor(t_1(x, y), t_2(x, y))) = T_1(p, q)T_2(p, q) \quad (8)$$

where F, G are the Fourier transform of f, g . It is a function of the relative position between the two functions and has application in pattern recognition and cryptanalysis.

We start with the simplest model for DS, a narrow vertical white slit on black background. The simulated PSD is in concordance with experimental and theoretical results. The next model consist of vertical or horizontal, equally distant, black and white stripe with different number of pixels and the simulated PSD is formed by a collinear points disposed horizontal or respectively vertical. For a black and white chess table, the PSD has the spots disposed at 45° . In all simple cases, the simulated PSD corresponds with theory and with experimental results.

We can inverse the problem and put in D plane the simulated diffractive pattern, and we study the correlation between these DS. On the SLM we must apply a phase matrix, so we transform the intensity distribution in phase distribution using the nonlinear dependence of phase with gray level (equations 4, 5, 6).

The experimental points for this SLM type [12] fitted by us with a 10-th order polynomial curved (polynomial coefficients are: $-1.4 \cdot 10^{-18}$, $1.8 \cdot 10^{-15}$, $-1 \cdot 10^{-12}$, $3.1 \cdot 10^{-10}$, $-5.6 \cdot 10^{-8}$, $6.3 \cdot 10^{-6}$, $-4.2 \cdot 10^{-4}$, $1.5 \cdot 10^{-2}$, $-2.6 \cdot 10^{-1}$, 1.6 , -2.9), introduces a nonlinear dependence emphasized by the correlation map (Fig. 5). Although coefficients of fitted curves are so small, a 9-th order polynomial fit introduces a great disagreement. We transformed the amplitude distribution in phase distribution in different ways: nonlinear polynomial dependence of 10-th order, linear dependence, and fractional dependence (Fig. 5).

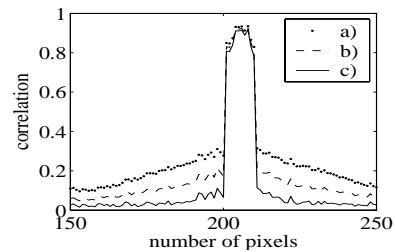


Fig. 5 Correlation between matrix with phase generated by IFTA and by a) 10-th order polynom, b) linear, c) fractional.

In that case we calculated the correlation function in D plane and complex maps with some symmetry (Fig. 6) are obtained. Again are relieved only vertical and horizontal peaks in map from letter O and also the diagonal peaks in map from letter A.

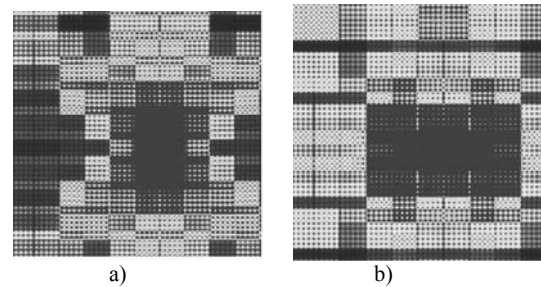


Fig. 6. Correlation maps between phase matrix in D plane from an array of a) letters A, b) letters O.

To study the next complicated correlation maps, we made some profiles after horizontal, vertical or diagonal rows. As expected, a strong spatial correlation exists between pixels where the same peaks in both matrixes are. When we add 4 pixels in standard letter A, the correlation is better than if we added 16 pixels and both are better than correlation between diffractive pattern from letter A and from letter O (Fig. 7).

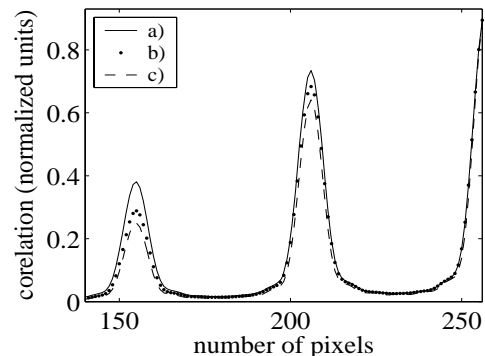


Fig. 7. A half from central profile of correlation map in E plane of two diffractive patterns from: a) standard letter A and standard letter A with 4 pixels add, b) standard letter A and standard letter A with 16 pixels add, c) standard letter A and letter O.

All these letters have the same size and periodicity and that thing is shown in the correlation profile, which follow the same shape, but with another magnitude. When we make the correlation between diffractive pattern from standard letter A and from standard letter A with different sizes, the correlation profile has another periodicity, magnitude, shape (Fig. 8). The same observation in case of a circle from points with size equal with all array O; correlation exists only in central area. The shape of DS is of less importance than the structure and size.

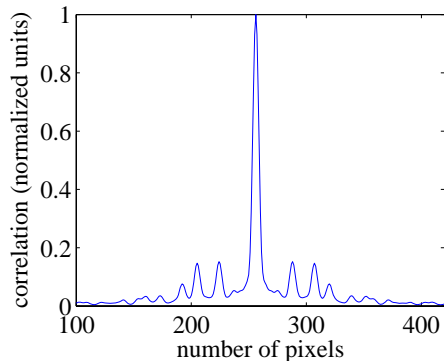


Fig. 8. Central profile of correlation map in E plane of two diffractive patterns from standard letter A and standard letter A with larger dimensions.

Starting with the diffractive pattern analysis, we model the DS with the aim to detect that DS which forms in E plane the diffractive pattern closer to the experimental one. We start a seeking algorithm based on the observation from simple models and the correlation between diffractive patterns. In the end we found a diffractive pattern with butterfly-like shapes for one model of letter A which we named the standard letter A, showing good agreement with the experimental one (Fig. 3a). Also the diffractive pattern from letter O with spots aligned in two vertical lines near the central spot, is obtained experimental (Fig. 3b) and by simulation (Fig. 9).

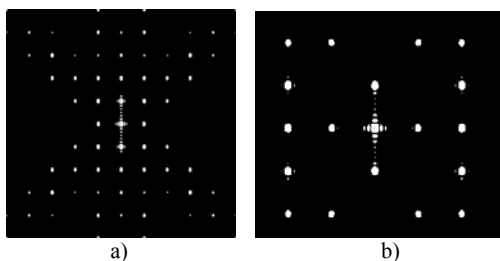


Fig. 9. Simulated PSD from letter a) A and b) O.

We observe in both images the horizontal and vertical arrangement of spots given by the arrangement of letters in rows and columns. In the PSD from letter A, we observe the arrangements of spots prevalent in a direction which

form an angle with the horizontal and vertical axis in concordance with the shape of letter A. In E plane, the sampling interval Δx is related with the dimension of the pixel from SLM plane $\Delta \tilde{x}$ by [13]: $N\Delta x\Delta \tilde{x} = \lambda L$, where pitch is $32\mu\text{m}$, and result for Δx in E plane 0.123mm for 5m between E and D plane. The positions of the diffraction maxima in E plane are calculated with the diffraction formula (we consider our array letter A like a multi-diffraction grating with different periods and tilts).

5. Discussion and conclusions

A bi-dimensional correlation is perfect where between two data sets exists a simple translation, a scale increase, a rotation from the origin or all three transformations combined. If in letter A exists another kind of changes (add or extract pixels from model), the diffractive patterns has small modification, hard to detect, but the profile of the correlation maps gave us information about them (recognizing objects having selected shapes and size and determining their coordinates). Correlation starting from DS with the same periodicity and size shows some overlapping peaks with other magnitude. When we modify periodicity or size, the profile of correlation map has peaks in different places. The shape of DS is of less importance than the structure and size.

The correlation maps are very complex but they follow a characteristic symmetric pattern. The optoelectronic spatial modulator is a useful device in such situation because we can obtain experimental diffractive pattern from our simulated DS and compare it to the desired one, from the natural or imprint objects. The phase factor is important in the SLM's function and the better between gray level and phase is the theoretical one.

The study of the simple models or text models is a start point from an algorithm which uses a diffractive pattern from the sample, like input data. Simulation model forms its diffractive pattern and the correlation between experimental and simulated diffractive patterns is calculated. Then in the simulation is changed the shape, size or structure of the DS, the correlation is again calculated and the algorithm is stopped when the correlation is obtained. The rule for changing the DS is based on observations of diffractive pattern from simple models and is perfectible.

As shown for operations with CGH, both letters A and O in D plane form on the E plane both diffractive patterns. Like a classical hologram, we can put on SLM a half or a quarter from CGH and the desired image appear in E plane. But when we add some periodical defects, the intensity in desired image is reduced proportionally.

References

- [1] X. Li, A. K. Soh, C. Huang, C. H. Yang, H. Shi, *Opt. Eng.* **41**(6), 1295 (2002).
- [2] Kishk, B. Javidi, *Opt. Expr.* **11**(26), 3528 (2003).
- [3] G. Wang, *Opt. Expr.* **14**(11), 4583 (2006).

- [4] A. Márquez, C. Iemmi, J. Campos, J. C. Escalera, M. J. Yzuel, *Opt. Epr.* **3**(3), 716 (2005).
- [5] Z. Cao, L. Xuan, L. Hu, Y. Liu, Q. Mu, D. Li, *Opt. Expr.*, **13**(4), 1059 (2005).
- [6] A. Márquez, C. Iemmi, I. Moreno, J. Campos, M. J. Yzuel, *Opt. Expr.* **13**(6), 2111 (2005).
- [7] J. W Goodman, Mc Graw-Hill Book Company, 1968, p. 52.
- [8] O. Ripoll, V. Kettunen, H. P. Herzig, *Opt. Eng.*, **43**(11), 2549 (2004).
- [9] D. C. O'Shea, T. J. Suleski, A. D. Kathman, D. W. Prather, Spie Press, Bellingham, Washington, USA, 2004, p. 96.
- [10] M. Mihailescu, L. Preda, Al. M. Preda, E. I. Scarlat, *U. P. B. Sci. Bull., Series A* **674**, 65 (2005).
- [11] A. Marquez, J. Campos, M. J. Yzuel, I. Moreno, J. A. Davis, C. Iemmi, A. Moreno, A. Robert, *Opt. Eng.* **39**(12), 3301 (2000).
- [12] V. Duran, J. Lancis, E. Tajahuerce, M. Fernandez-Alonso, *Opt. Exp.* **14**, 5607 (2006).
- [13] J. Garcia, D. Mas, R. G. Dorsch, *Appl. Opt.* **35**(35), 7013 (1996).

*Corresponding author: mona_m@physics.pub.ro